Journal of Solid State Chemistry 184 (2011) 2196–2203

Contents lists available at ScienceDirect

Journal of Solid State Chemistry

journal homepage: www.elsevier.com/locate/jssc

Metal-organic framework based on copper(I) sulfate and 4,4′-bipyridine catalyzes the cyclopropanation of styrene

Fa-Nian Shi *, Ana Rosa Silva *, João Rocha

Department of Chemistry, CICECO, University of Aveiro, 3810-193 Aveiro, Portugal

ARTICLE INFO

Article history:
Received 11 January 2011
Received in revised form
14 June 2011
Accepted 22 June 2011
Available online 29 June 2011

Keywords:
Metal organic framework
Cu(I)
4,4′-bipyridine
Sulfate
Heterogeneous catalysis

ABSTRACT

The hydrothermal synthesis of a new metal-organic framework (MOF) formulated as Cu_2(4,4′-bpy)$_2SO_4 \cdot 6(H_2O)$, [abbreviation: (1); bpy or 4,4′-bpy=4,4′-bipyridine; SO_4^{2-}=sulfate group] has been reported. The structure of this MOF consists of Cu^+ nodes connected via 4,4′-bpy to form infinite chains, with two neighboring chains further bridged on the nodes by SO_4^{2-}, resulting in a 1-D double chain network. Guest water molecules reside in between the chains and are hydrogen-bonded to the O and S atoms from the nearest sulfate groups, leading to the formation of a 3-D supramolecular framework. This MOF is good heterogeneous catalyst for the cyclopropanation of styrene, with high *trans* cyclopropane diastereoselectivity and was recycled and reused for three consecutive cycles without a significant loss of catalytic activity.

1. Introduction

Metal organic frameworks (MOFs) [1–5] with both organic and inorganic ligands are a type of well-crystallized hybrid materials [6–8]. Recently these materials have been the subject of increasing studies as potential functional materials owing to their inorganic structural features analog to those of metal oxides being tuned with the addition of various organic ligands, leading to the improvement of their original properties. Copper(I) (Cu^+) ions possesses a filled 3d shell, thus showing diamagnetic and photo-luminescent properties [9] with the well known MLCT (metal–ligand charge transfer) mechanism. But inorganic cuprous salts, such as cuprous sulfate, are usually unstable in air and are easily converted into cupric salts in the presence of water or moisture, and so some organic species (*e.g.* bpy or phen) may be used to stabilize cuprous salts and enhance the initial properties of the inorganic cuprous salts.

In fact, the SO_4^{2-} group is a good linker, which can donate its one [10–13], two [14–17], three [6,18–20] and even four [21–23] oxygen atoms to connect to metals. Hence, the SO_4^{2-} group is a good candidate for building novel 'hybrid' MOFs, with mixed organic and inorganic linkers. Copper(I) can adopt 3 [24,25] and 4 [14,26] coordination numbers with N-containing bridging ligands into catena polymeric frameworks. There are several reports on the Cu-(4,4′-bpy)-SO_4 system, but most deal with Cu(II) [16,27–31]. Only two reports [16,32] are available on 'hybrid' MOFs containing Cu(I), which were synthesized under solvothermal (methanol) synthetic conditions at relatively high temperature ($\geq 140\ ^\circ C$).

Since MOFs are crystalline coordination polymers constituted by networks of metal ions held in place by multidentate organic molecules, one of their potential applications is catalysis. They can be regarded as self supported coordination compounds and, therefore, may act as heterogeneous catalysts in organic transformations. However, the use of MOFs as heterogeneous catalysts is an area that is still in its infancy [33]. Several monomeric coordination copper(I) complexes with nitrogen ligands are active homogeneous catalysts in the cyclopropanation of alkenes [34,35]. Cyclopropanes are versatile organic compounds, which may be converted into a variety of useful products by cleavage of the strained three-membered ring [35].

Herein, we report a new hybrid MOF in the Cu^+-(4,4′-bipyridine)-SO_4 system, prepared under hydrothermal conditions with aspartic acid as the reducing agent, with a monoclinic and relatively large unit cell volume ($> 10{,}000\ Å^3$). The single-crystal structure database (WebCSD v1.1.1, updated on 2010.10.20) contains a single compound [36] with similar unit cell parameters. The new Cu(I) MOF (1) was applied as a heterogeneous catalyst in the cyclopropanation of styrene.

2. Experimental

2.1. Materials

All reagents are commercially available and were used without further purification. Copper (II) sulfate 5-hydrate ($CuSO_4 \cdot 5\ H_2O$,

* Corresponding authors.
E-mail addresses: fshi@ua.pt (F.-N. Shi), ana.rosa.silva@ua.pt (A.R. Silva).

0022-4596/$ - see front matter © 2011 Elsevier Inc. All rights reserved.
doi:10.1016/j.jssc.2011.06.023

≥99.5%, Panreac), 4,4′-bipyridine (4,4′-bpy, $C_{10}H_8N_2$, ≥98%, Alfa Aesar), L-aspartic acid (L-asp, $C_4H_7NO_4$, ≥99%, BDH biochemicals). Copper(II) trifluoromethanosulfonate ([$Cu(Otf)_2$]), 2,2-Bis[2-(4(*S*)-tert-butyl-1,3-oxazolinyl)]propane (Box), styrene, *n*-undecane, ethyldiazoacetate and phenylhydrazine were purchased from Aldrich and dichloromethane from Romil.

2.2. $Cu_2(4,4'\text{-bpy})_2SO_4\cdot 6(H_2O)$, (1)

0.1153 g (0.46 mmol) of copper sulfate, 0.1030 g (0.66 mmol) of 4,4′-bpy and 0.0787 g (0.59 mmol) of L-asp were added into 16 mL of distilled water under magnetic stirring. The mixture was transferred into a 40 mL Teflon-lined autoclave and heated at 120 °C in an oven for 3 days. After natural cooling, the sample was filtered and washed with 3×50 mL distilled water. Greenish yellow crystals of (1) were obtained as a pure phase and air-dried at ambient conditions (0.08 g, yield *ca.* 54% based on $CuSO_4$). IR data: 3445 (b), 1630 (m), 1601(s), 1527 (m), 1486 (s), 1409 (s), 1218 (m), 1104 (s), 795 (m), 721 (w), 621 (m), 472 (m).

2.3. Instrumentation

Powder X-ray diffraction data (PXRD) were collected at ambient temperature (*ca.* 298 K) on a X'Pert MPD Philips diffractometer (Cu-*K*α radiation, $\lambda=1.54056$ Å), equipped with a X'Celerator detector, curved graphite monochromated radiation and a flat-plate sample holder, in a Bragg–Brentano para-focusing optics configuration (40 kV, 50 mA). Intensity data were collected in the continuous scanning mode in the range ca. $5^\circ<2\theta<50^\circ$. FTIR spectra were collected using KBr pellets (Aldrich, 99%+, FTIR grade) on a Mattson 7000 FTIR spectrometer. Thermogravimetric analysis (TGA) was carried out on a Shimadzu TGA-50, between room temperature and 700 °C with a heating rate of 5 °C/min, under an air atmosphere, respectively, with a flow rate of 20 cm^3/min. Scanning electron microscopy (SEM) was performed using a Hitachi Su-70 and energy dispersive analysis of X-rays spectroscopy (EDS) was carried out on a Bruker QUANTAX 400 instruments working at 15 kV. Samples were prepared by deposition on aluminum sample holders by carbon coating.

2.4. Catalysis experiments

The catalytic activity of the Cu(I) MOF in the cyclopropanation of styrene was tested at room temperature in batch reactors at atmospheric pressure, with and without constant magnetic stirring. Typically, 5.00 mmol of styrene, 1.80 mmol of *n*-undecane and 0.139 g of (1) in 10.0 ml of dichloromethane were used. Finally, 0.65 ml of ethyldiazoacetate (EDA) was added to the reaction mixture at a rate 0.32 ml/h over 2 h using a syringe pump. When the addition of ethyldiazoacetate finished, aliquots (0.05 ml) were periodically withdrawn from the reaction mixture with a hypodermic syringe, filtered through PTFE 0.2 μm syringe filters, and analyzed by GC-FID by the internal standard method. At the end of the reactions, the solution was removed with a syringe and then (1) was washed several times with fresh dichloromethane, dried in air overnight and reused in another cycle using the same experimental procedure.

In order to compare with the heterogeneous phase reactions, three homogeneous phase control experiments were also performed using this experimental procedure and: 0.0071 g of 4,4-bpy (0.045 mmol) and 0.0112 g of copper(II) sulfate (0.045 mmol); 1.0% mol of [$Cu(Otf)_2$] and Box and, finally, no catalyst. Although the Cu(II) complex with Box is also highly active in the cyclopropanation of styrene, phenylhydrazine was added to solution in order to reduce the Cu(II) homogeneous complex to Cu(I).

The reaction mixture was analyzed by GC-FID (using the internal standard method) on a Varian 450 GC gas chromatograph equipped with a fused silica Varian Chrompack capillary column CP-Sil 8 CB Low Bleed/MS (15 m × 0.25 mm id; 0.15 μm film thickness), using helium as carrier gas. Conditions used: 125 °C (40 min); injector temperature, 200 °C; detector temperature, 250 °C. The several chromatographic peaks were identified against commercially available samples and/or by GC–MS (Finnigan Trace).

2.5. X-ray crystallography

Complete single-crystal data were collected at 150(2) K on a Bruker X8 Kappa APEX II charge-coupled device (CCD) area-detector diffractometer (Mo-*K*α graphite monochromated radiation, $\lambda=0.7107$ Å) controlled by the APEX2 software package [37] and equipped with an Oxford Cryosystems Series 700 cryostream monitored remotely using the software interface Cryopad [38]. Images were processed using the software package SAINT+ [39]. Absorption corrections were applied by the multiscan semiempirical method implemented in SADABS [40]. The structure was solved by direct method using SHELXS-97 [41] and refined using SHELXL-97 [42]. All non-hydrogen atoms were successfully refined with anisotropic displacement parameters. Hydrogen atoms bound to carbon were located at their idealized positions by employing the HFIX 43 instruction in SHELXL-97 and included in subsequent refinement cycles in riding motion approximation with isotropic thermal displacement parameters (U_{iso}) fixed at 1.2 Ueq of the carbon atom to which they were attached. The hydrogen atoms associated with water molecules were visible in the last difference Fourier maps synthesis. These atoms have been included in the final structural models with the O–H distances restrained to 0.82(1) Å, in order to ensure a chemically reasonable geometry for these moieties, and with U_{iso} fixed at 1.2 Ueq of the parent oxygen atoms. The detailed crystallographic data and structural refinement parameters have been summarized in Table 1. Complete crystallographic data for the structure reported in this paper have been deposited in the CIF

Table 1
Summary of crystal data and structure refinement for (1).

Compound	(1)
T (K)	150
Formula	$C_{20}H_{28}Cu_2N_4O_{10}S$
FW	643.60
Space group	*P*2(1)/*c*
a (Å)	29.107(2)
b (Å)	17.1516(12)
c (Å)	21.5943(15)
β (deg.)	110.371(3)
V (Å)^3	10106.1(12)
Z	16
Dc (g cm^{-3})	1.692
Absorption coefficient μ (mm^{-1})	1.827
Crystal size (mm^3)	0.22×0.20×0.08
Theta range for data collection	3.56 to 30.51
Index ranges	$-41\le h\le 41$, $-24\le k\le 22$, $-30\le l\le 30$
Reflections collected	178,549
Independent reflections	30,804 [*R*(int)=0.0555]
Completeness to theta	99.8%
R_{int}	0.0555
Data/restraints/parameters	30,804/45/1459
Final *R*[*I* > 2sigma(*I*)]	*R*1=0.0524, w*R*2=0.1197
R indices (all data)	*R*1=0.0914, w*R*2=0.1376
GOF	1.018
Δρmax (min/e Å^{-3})	1.669 and −0.824

format with the Cambridge Crystallographic Data Center as supplementary publication no. CCDC 805893. Copies of the data can be obtained free of charge on application to CCDC, 12 Union Road, Cambridge CB2 1EZ, UK (fax: (44) 1223336-033; e-mail: hdeposit@ccdc.cam.ac.uk).

3. Results and discussion

Compound (1) was synthesized via a mild hydrothermal reaction using aspartic acid as a reductant. This synthetic strategy shows that an appropriate reducing agent can easily reduce Cu(II) to Cu(I) under hydrothermal conditions at relatively low temperature (120–130 °C). The final product exhibits the large particles shown in Fig. 1, being most of them visible by naked eye. The SEM image of the particles shows the species are formed irregularly and usually aggregated into big polycrystalline particles, however, it is possible to find out smaller and qualified single crystals for characterization. EDS analyses by point method on the three surface spots of the different crystalline particles for the same sample give the similar molar ratio Cu:*S*=69:31 (66:34; 68:32) ≈ 2:1 indicating that Cu here is Cu(I), for charge balance, which is consistent with the single crystal structure data.

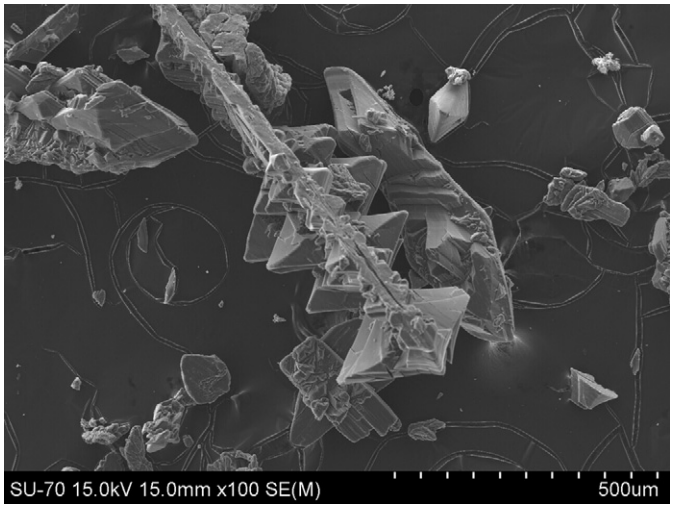

Fig. 1. SEM image of the crystalline particles of (1).

3.1. Structure description

Compound (1) forms an infinite double chain network similar to the one reported in literature [16], which possesses the same secondary building unit $[Cu_2(SO_4)(4,4'\text{-bpy})_2]$. However, the unit cell volume of (1) is much larger and the asymmetric unit contains eight crystallographic unique Cu sites and twenty-four guest water molecules $[Cu_2(SO_4)(4,4'\text{-bpy})_2]_4 \cdot 24H_2O$ (Fig. 2) while there are only two crystallographic independent Cu sites in the material quoted in [16]. In Fig. 3, each crystallographic independent copper has similar coordination geometry and chemical environment. In fact, all copper atoms coordinate to two nitrogen atoms from 4,4′-bpy with the bonding distances varying from 1.900(2) to 1.922(2) Å and one oxygen atom from a sulfate group with the bonding distances changing from 2.257(2) to 2.359 Å (Table 2), which are longer than the Cu–N distances. Therefore, each copper is linked via 4,4′-bpy into an infinite chain, while sulfate groups bridge two neighboring chains via copper nodes into an infinite double chain network. The rings of 4,4′-bpy molecules are somewhat distorted from the plane, the torsion angles as labeled in Fig. 3 have been included in Table 2. Nevertheless, the two opposite rings from 4,4′-bpy molecules within the double chains are roughly parallel with the face to face distances of *ca.* 3.5 Å suggesting π–π stacking interaction between aromatic rings (Fig. 3).

Fig. 4 shows how the infinite chains pack in the structure. As previously reported [16], the double chains consisting of copper, 4,4′-bpy and sulfate groups are further assembled into layers, with no direct interaction with each other, parallel to the *a*–*c* planes (Fig. 4) with the sulfate groups protruding up-and-down

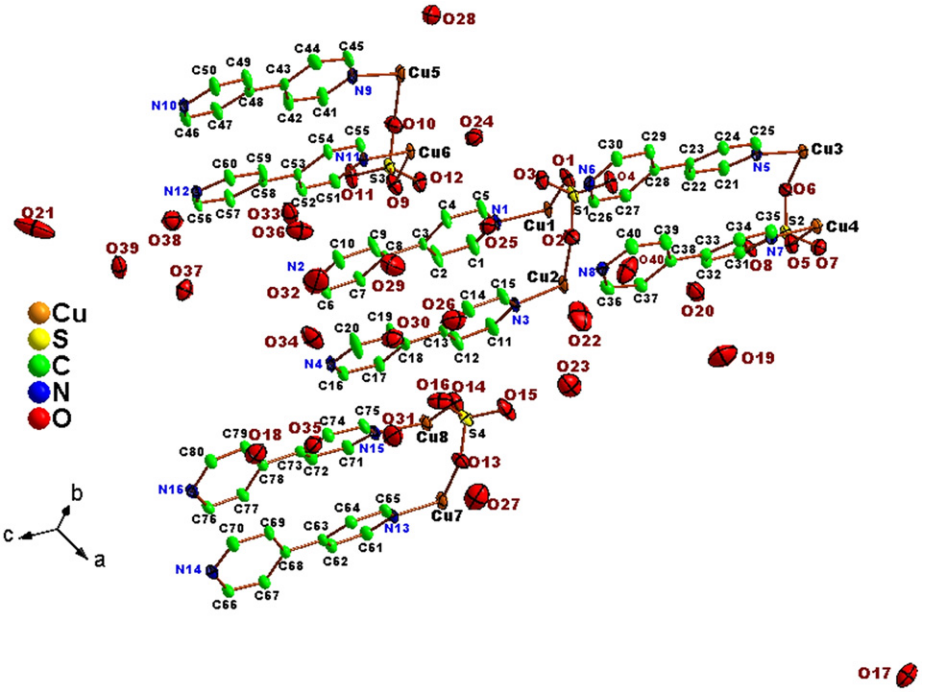

Fig. 2. Asymmetric unit of (1) contains eight crystallographically independent Cu^+ ions, four SO_4^{2-} fragments and twenty-four water guest molecules. The labeling scheme for all non-hydrogen atoms are shown. Atoms are drawn as thermal ellipsoids at the 50% probability level. Hydrogen atoms are omitted for clarity.

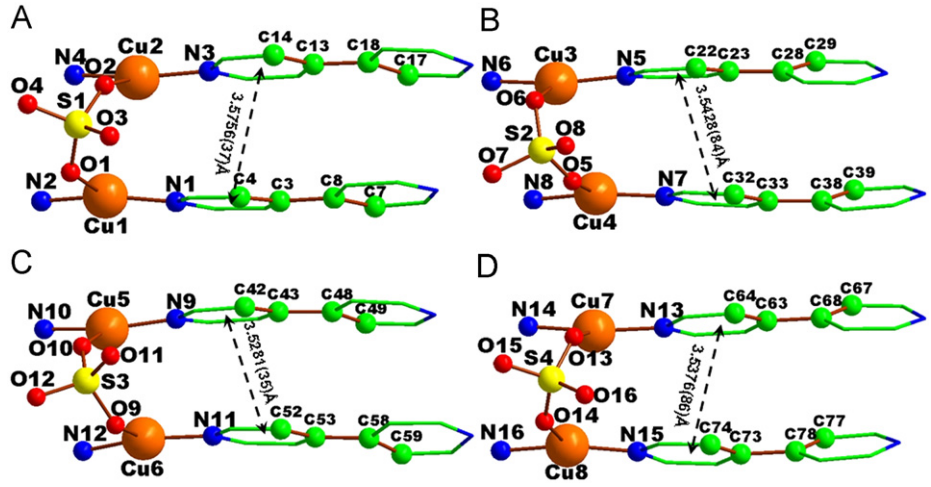

Fig. 3. Ball-and-stick view of the copper coordination environments and the secondary building unit indicating π–π interaction between the aromatic rings of 4,4′-bpy (distances are depicted close to the arrows pointing to the centers of the aromatic rings).

Table 2
Selected bond distances (Å), angles (deg.) and the torsion angles (deg.) for (1).

Cu(1)–N(1)	1.900(2)	Cu(1)–N(2)#1	1.904(2)	Cu(1)–O(1)	2.359(2)
Cu(2)–N(4)#1	1.914(2)	Cu(2)–N(3)	1.922(2)	Cu(2)–O(2)	2.281(2)
Cu(3)–N(6)#2	1.910(2)	Cu(3)–N(5)	1.916(2)	Cu(3)–O(6)	2.257(2)
Cu(4)–N(8)#2	1.900(3)	Cu(4)–N(7)	1.912(2)	Cu(4)–O(5)	2.273(2)
Cu(5)–N(9)	1.906(2)	Cu(5)–N(10)#2	1.915(2)	Cu(5)–O(10)	2.262(3)
Cu(6)–N(12)#2	1.908(2)	Cu(6)–N(11)	1.912(2)	Cu(6)–O(9)	2.261(2)
Cu(7)–N(14)#1	1.900(3)	Cu(7)–N(13)	1.907(2)	Cu(7)–O(13)	2.334(2)
Cu(8)–N(15)	1.906(2)	Cu(8)–N(16)#1	1.910(2)	Cu(8)–O(14)	2.334(2)
S(1)–O(4)	1.466(2)	S(1)–O(2)	1.474(3)	S(1)–O(3)	1.476(2)
S(1)–O(1)	1.481(3)	S(2)–O(8)	1.464(2)	S(2)–O(7)	1.480(2)
S(2)–O(6)	1.482(2)	S(2)–O(5)	1.483(2)	S(3)-O(11)	1.466(2)
S(3)–O(10)	1.468(3)	S(3)–O(12)	1.473(2)	S(3)–O(9)	1.487(3)
S(4)–O(16)	1.463(3)	S(4)–O(15)	1.471(3)	S(4)–O(13)	1.476(3)
S(4)–O(14)	1.481(3)	N(1)–Cu(1)–N(2)#1	163.08(11)	N(1)–Cu(1)–O(1)	99.28(9)
N(2)#1–Cu(1)–O(1)	97.01(9)	N(4)#1–Cu(2)–N(3)	160.27(12)	N(4)#1–Cu(2)–O(2)	100.36(11)
N(3)–Cu(2)–O(2)	98.60(10)	N(6)#2–Cu(3)–N(5)	161.14(11)	N(6)#2–Cu(3)–O(6)	99.36(10)
N(5)–Cu(3)–O(6)	98.96(10)	N(8)#2–Cu(4)–N(7)	161.90(11)	N(8)#2–Cu(4)–O(5)	101.59(10)
N(7)–Cu(4)–O(5)	95.94(10)	N(9)–Cu(5)–N(10)#2	159.96(12)	N(9)–Cu(5)–O(10)	100.67(11)
N(10)#2–Cu(5)–O(10)	98.94(11)	N(12)#2–Cu(6)–N(11)	160.51(11)	N(12)#2–Cu(6)–O(9)	100.63(10)
N(11)–Cu(6)–O(9)	98.22(9)	N(14)#1–Cu(7)–N(13)	163.67(12)	N(14)#1–Cu(7)–O(13)	98.44(10)
N(13)–Cu(7)–O(13)	96.98(10)	N(15)–Cu(8)–N(16)#1	162.62(12)	N(15)–Cu(8)–O(14)	101.11(10)
N(16)#1–Cu(8)–O(14)	95.64(10)	O(4)–S(1)–O(2)	109.06(16)	O(4)–S(1)–O(3)	109.77(14)
O(2)–S(1)–O(3)	109.26(14)	O(4)–S(1)–O(1)	109.68(14)	O(2)–S(1)–O(1)	109.80(15)
O(3)–S(1)–O(1)	109.25(15)	O(8)–S(2)–O(7)	110.21(14)	O(8)–S(2)–O(6)	110.05(14)
O(7)–S(2)–O(6)	108.64(13)	O(8)–S(2)–O(5)	109.83(13)	O(7)–S(2)–O(5)	108.63(14)
O(6)–S(2)–O(5)	109.46(14)	O(11)–S(3)–O(10)	109.37(18)	O(11)–S(3)–O(12)	109.97(15)
O(10)–S(3)–O(12)	109.08(15)	O(11)–S(3)–O(9)	109.69(15)	O(10)–S(3)–O(9)	109.80(16)
O(12)–S(3)–O(9)	108.91(15)	O(16)–S(4)–O(15)	110.93(19)	O(16)–S(4)–O(13)	108.69(15)
O(15)–S(4)–O(13)	108.78(17)	O(16)–S(4)–O(14)	108.64(16)	O(15)–S(4)–O(14)	109.97(16)
O(13)–S(4)–O(14)	109.82(15)	S(1)–O(1)–Cu(1)	129.95(14)	S(1)-O(2)–Cu(2)	138.30(17)
S(2)–O(5)–Cu(4)	144.54(15)	S(2)–O(6)–Cu(3)	122.38(14)	S(3)–O(9)–Cu(6)	124.18(15)
S(3)–O(10)–Cu(5)	145.69(19)	S(4)–O(13)–Cu(7)	128.07(15)	S(4)–O(14)–Cu(8)	139.68(16)
Selected torsion angles (deg.)					
C(4)–C(3)–C(8)–C(7)	173.9(3)	C(14)–C(13)–C(18)–C(17)	175.3(3)	C(22)–C(23)–C(28)–C(29)	−162.6(3)
C(32)–C(33)–C(38)–C(39)	−157.2(3)	C(42)–C(43)–C(48)–C(49)	170.8(3)	C(52)–C(53)–C(58)–C(59)	169.3(3)
C(64)–C(63)–C(68)–C(67)	−153.7(3)			C(74)–C(73)–C(78)–C(77)	−150.6(3)

Symmetry transformations used to generate equivalent atoms: #1 x, $-y+1/2$, $z-1/2$; #2 x, $-y+3/2$, $z-1/2$.

into the interlayer space. Almost all coordinated and uncoordinated oxygen atoms from these sulfate groups form complicated hydrogen-bonding networks with a variety of guest water molecules as shown in Fig. 5.

In order to highlight the hydrogen bonding networks in (1), the copper and 4,4′-bpy have been removed from Fig. 5 and the structure rotated by 90°, giving Fig. 6 showing a hydrogen bonding interaction plane. This plane consists of two chains self-assembled by the lattice water guests further linking together via sulfate groups as bridges extending into an infinite plane by hydrogen bonding (Fig. 6 and Table 3), eventually leading to the formation of a supramolecular 3-D framework of (1).

3.2. Thermal properties

The thermal stability of (1) was studied in air from room temperature to 700 °C. In this range, the TGA plot of (1) exhibits several weight loss steps due to the removal of lattice water and

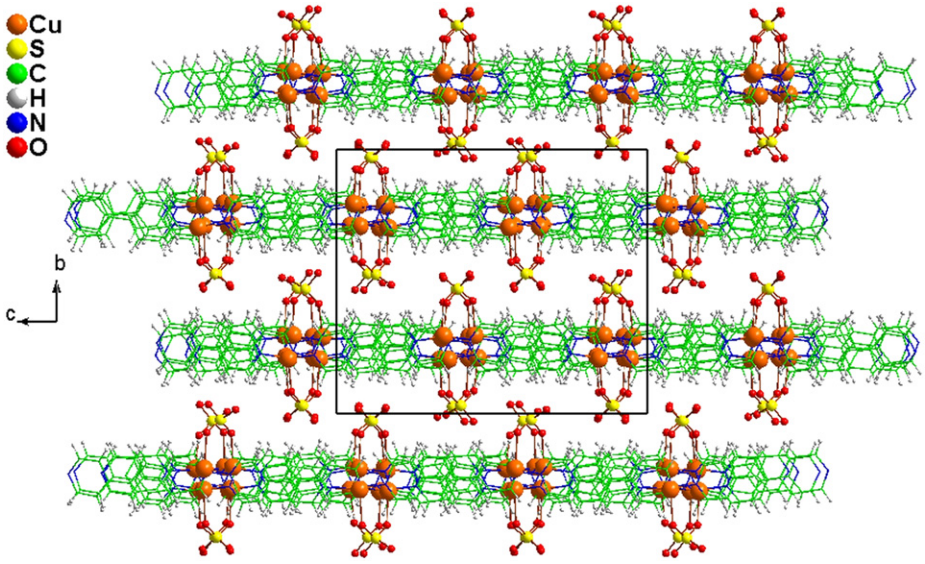

Fig. 4. Packing diagram of (1) viewing along *a* axis showing bonded sulfate groups from different chains layers protruding up-and-down into the interlayer space. Guest water molecules in between the layers are omitted for clarity.

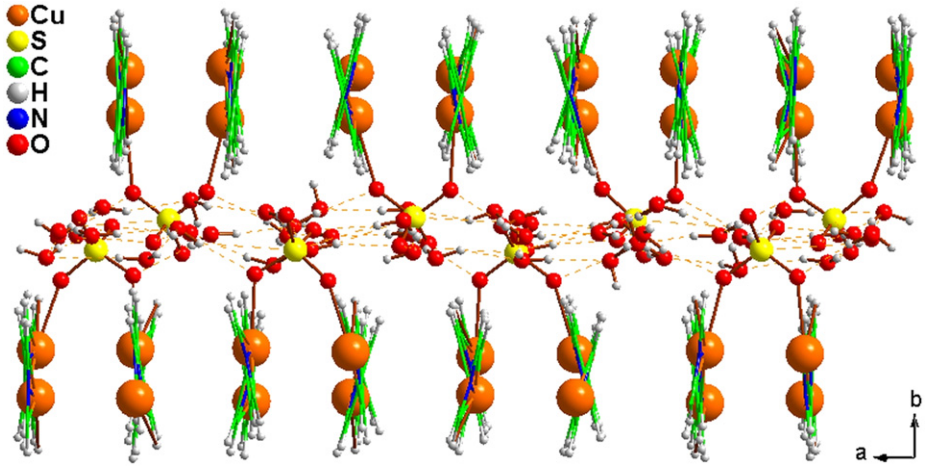

Fig. 5. Ball-and-stick representation of the unit cell of (1) viewed along the c axis. C and N are displayed in wireframe. Hydrogen bonding among guest water molecules and sulfate groups between the double chains are depicted by dotted lines, and lead to the formation of a 3-D supramolecular framework.

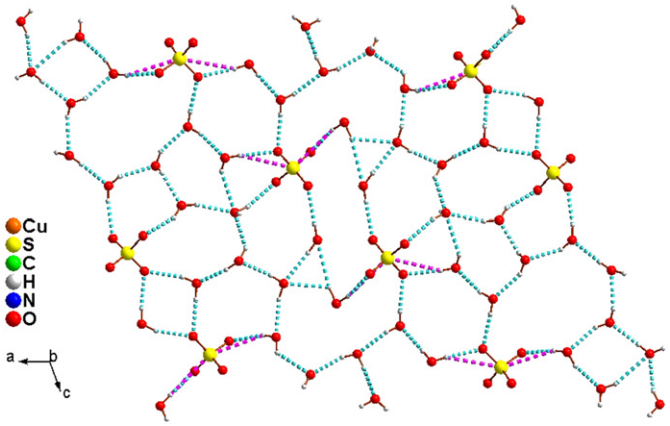

Fig. 6. Network of hydrogen bonding among water guests and sulfate groups to form an infinite layer. H···O bonds are depicted in cyan, while the H···S bonds are colored in pink for clarity. (For interpretation of the references to color in this figure legend, the reader is referred to the web version of this article.)

4,4′-bpy molecules (Fig. 7). From room temperature to 100 °C, only partial (*ca.* 10%) water is released that is comparable with the thermal behaviors reported in literatures [25,27,31] indicating the different stability of the lattice water molecules with comprehensive hydrogen bonding interaction, while the full removal of the guest water molecules occurs at *ca.* 195 °C. The total amount of 16.99% of all water molecules are removed from the lattice, which is consistent with the calculated value of 16.78% due to breaking of hydrogen bonding interaction. From 195 to 460 °C the plot is composite, suggesting that the loss of 4,4′-bpy is complex possibly due to the presence of several different coordination environment for 4,4′-bpy. The total weight loss of 50.00% from 195 to 460 °C is in fair agreement with the calculated value of 48.48% due to decomposition of the network and releasing of the 4,4′-bpy molecules that is similar to the thermal decomposition temperature of 4,4′-bpy reported in the literature [25,31] but different from that of [27] in which the study was performed under nitrogen atmosphere. Although there is no weight loss from 460 to 600 °C, above 600 °C there is again new weight loss due to

Table 3
Hydrogen bonds for (1).

D–H…A	d(D–H)	d(H…A)	d(D…A)	<(DHA)
O(17)–H(17A)…O(10)#5	0.813(19)	2.24(2)	3.040(5)	167(5)
O(17)–H(17A)…S(3)#5	0.813(19)	2.96(4)	3.629(3)	142(5)
O(17)–H(17B)…O(33)#6	0.812(19)	1.94(2)	2.753(5)	176(6)
O(18)–H(18A)…O(35)	0.808(19)	2.20(4)	2.852(4)	137(5)
O(18)–H(18B)…O(5)#7	0.829(19)	2.01(2)	2.832(4)	171(5)
O(18)–H(18B)…S(2)#7	0.829(19)	3.00(3)	3.775(3)	157(5)
O(19)–H(19A)…O(20)	0.82(2)	1.92(3)	2.709(5)	161(7)
O(19)–H(19B)…O(18)#8	0.83(2)	2.06(3)	2.855(6)	162(8)
O(20)–H(20A)…O(8)	0.83	2.15	2.765(4)	131.1
O(21)–H(21A)…O(28)#4	0.78(2)	2.09(3)	2.824(7)	155(7)
O(21)–H(21B)…O(1)#7	0.80(2)	2.02(3)	2.814(5)	168(8)
O(21)–H(21B)…S(1)#7	0.80(2)	2.99(3)	3.770(4)	165(7)
O(22)–H(22A)…O(36)#2	0.82(2)	1.94(2)	2.755(7)	171(8)
O(22)–H(22B)…O(40)	0.87(2)	2.02(3)	2.872(7)	167(7)
O(23)–H(23A)…O(15)	0.85	2.06	2.909(5)	179.8
O(23)–H(23B)…O(22)	0.84	2.07	2.910(7)	177.7
O(24)–H(24A)…O(3)	0.833(19)	2.00(2)	2.809(4)	162(4)
O(24)–H(24B)…O(12)	0.830(19)	1.99(2)	2.812(4)	172(5)
O(25)–H(25A)…O(12)	0.825(19)	2.05(2)	2.848(4)	164(4)
O(25)–H(25B)…O(3)	0.850(19)	1.97(2)	2.814(4)	170(4)
O(26)–H(26B)…O(14)	0.82(2)	2.10(3)	2.891(5)	163(6)
O(27)–H(27A)…O(22)#6	0.965(19)	2.40(5)	2.992(7)	119(4)
O(27)–H(27A)…O(23)#6	0.965(19)	2.56(2)	3.509(5)	167(4)
O(27)–H(27B)…O(13)	0.895(19)	1.95(2)	2.833(5)	169(5)
O(27)–H(27B)…S(4)	0.895(19)	2.91(4)	3.710(4)	150(5)
O(28)–H(28A)…O(38)#2	0.806(19)	1.95(2)	2.750(5)	171(6)
O(28)–H(28B)…O(24)#9	0.824(19)	1.94(2)	2.749(5)	167(6)
O(29)–H(29A)…O(26)	0.81(2)	2.07(3)	2.852(6)	163(8)
O(29)–H(29B)…O(9)	0.81(2)	2.05(4)	2.804(5)	154(7)
O(30)–H(30A)…O(16)	0.820(19)	2.01(2)	2.804(4)	164(5)
O(30)–H(30A)…S(4)	0.820(19)	2.96(3)	3.729(3)	157(5)
O(30)–H(30B)…O(26)	0.811(19)	2.34(4)	3.027(6)	143(5)
O(31)–H(31A)…O(16)	0.821(19)	1.98(3)	2.771(4)	163(6)
O(31)–H(31B)…O(19)#6	0.808(19)	1.98(3)	2.715(6)	150(6)
O(32)–H(32A)…O(34)	0.83(2)	1.95(4)	2.716(6)	153(8)
O(32)–H(32B)…O(29)	0.83(2)	2.08(7)	2.712(7)	133(8)
O(33)–H(33A)…O(11)	0.812(19)	1.99(2)	2.789(4)	170(5)
O(33)–H(33B)…O(32)	0.780(19)	2.00(3)	2.699(6)	150(5)
O(34)–H(34A)…O(30)	0.843(19)	2.00(2)	2.824(5)	165(5)
O(34)–H(34B)…O(7)#7	0.827(19)	1.95(2)	2.775(4)	174(5)
O(35)–H(35A)…O(7)#7	0.815(19)	1.98(2)	2.786(4)	173(5)
O(35)–H(35A)…S(2)#7	0.815(19)	3.00(3)	3.748(3)	154(4)
O(35)–H(35B)…O(31)	0.816(19)	1.96(2)	2.781(5)	178(5)
O(36)–H(36A)…O(25)#4	0.849(19)	1.92(2)	2.763(5)	169(6)
O(36)–H(36B)…O(26)#4	0.82(2)	2.13(4)	2.792(6)	138(5)
O(37)–H(37A)…O(6)#7	0.844(19)	2.00(2)	2.833(4)	170(5)
O(37)–H(37A)…S(2)#7	0.844(19)	2.96(3)	3.683(3)	146(4)
O(37)–H(37B)…O(39)	0.850(19)	1.97(2)	2.793(4)	162(5)
O(38)–H(38A)…O(17)#6	0.768(18)	2.05(3)	2.768(5)	155(5)
O(38)–H(38B)…O(37)	0.781(18)	2.00(2)	2.737(4)	158(5)
O(39)–H(39A)…O(4)#7	0.847(19)	1.87(2)	2.714(4)	173(5)
O(39)–H(39A)…S(1)#7	0.847(19)	2.94(2)	3.749(3)	162(4)
O(39)–H(39B)…O(28)#4	0.832(19)	2.40(3)	3.188(5)	158(4)
O(40)–H(40A)…O(20)	0.83	2.31	2.810(5)	119.0
O(40)–H(40B)…O(2)	0.83	2.07	2.877(4)	162.3
O(40)–H(40B)…S(1)	0.83	3.01	3.675(4)	138.2

Symmetry transformations used to generate equivalent atoms: #1x, $-y+1/2$, $z-1/2$; #2 x, $-y+3/2$, $z-1/2$; #3 x, $-y+1/2$, $z+1/2$; #4 x, $-y+3/2$, $z+1/2$; #5$x+1$, y, z; #6 $-x+1$, $-y+1$, $-z+1$; #7x, y, $z+1$; #8 x, y, $z-1$; #9$-x$, $y+1/2$, $-z+1/2$.

the complicated decomposition of the sulfate groups and oxidation–reduction of cuprous ion [25], which will not be discussed here.

3.3. Catalytic studies

The purity of the bulk sample (1) for catalytic studies was proved via PXRD analysis (Fig. 8). After 45 min of addition of EDA at 0.32 ml/h rate to the solution containing styrene and (1), strong liberation of nitrogen gas was observed at the surface of the MOF

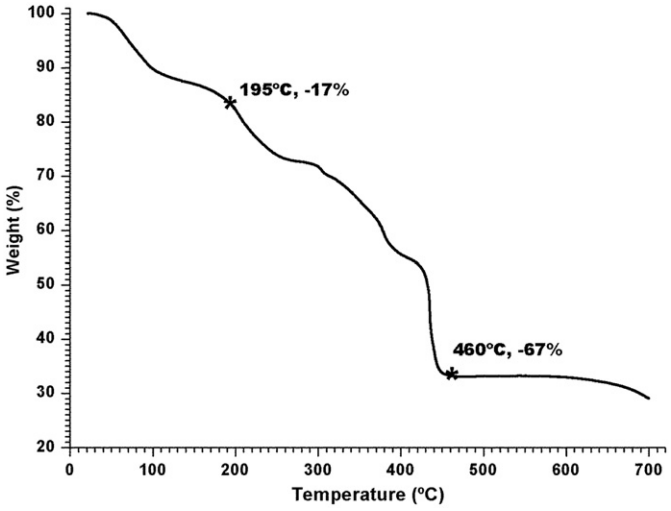

Fig. 7. Thermogram of (1) in air.

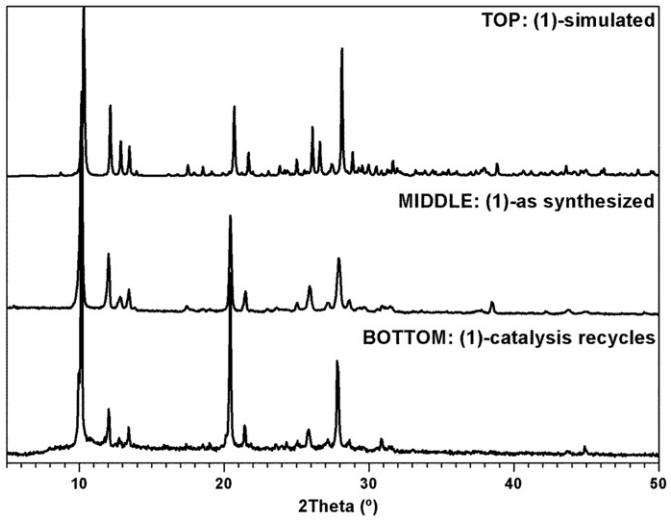

Fig. 8. PXRD patterns of (1). Top: simulated from single crystal data; middle: experimental pattern of the as-synthesized sample; bottom: experimental pattern after four catalytic cycles.

crystals, the by-product of the cyclopropanation reaction (Fig. 9). A 20% conversion of styrene into cyclopropane after 24 h was detected by GC with 72%, *trans* diastereoselectivity, slightly higher than in the homogeneous phase reaction with the best catalyst available (CuBox) for this reaction (Table 4). Likewise to this homogeneous catalyst [34], the cyclopropanation actives sites in the MOF are the copper(I) centres with N_2O_2 coordination sphere, from two independent 4,4′-bipyridine molecules and two sulphate molecules. Although the mechanism of the copper catalyzed cyclopropanation reactions is still not fully understood it is generally accepted that this reaction proceeds via a copper–carbene complex formed upon coordination of the EDA and consequent loss of nitrogen [43]. Hence the MOF copper(I) centre has still free coordination sites and allows the formation of the carbene intermediate.

In the second cycle the liberation of nitrogen was not as strong as in the first catalytic cycle and the reaction took twice the time to achieve a comparable styrene conversion (23%), although with the same diastereoselectivity (72%). In the 3rd cycle the strong liberation of nitrogen was again observed and the styrene conversion obtained in 24 h was similar to that of the 1st cycle, with

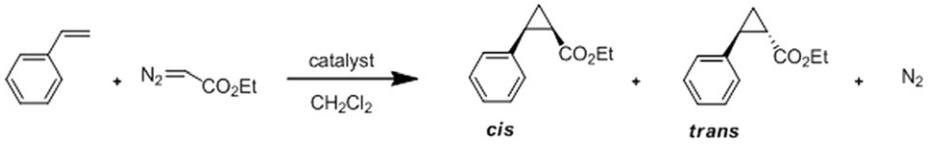

Fig. 9. Cyclopropanation of styrene with ethyldiazoacetate.

Table 4
Results of the cyclopropanation of styrene with EDA using the Cu(I) MOF as catalyst.[a]

	Run	t (h)	%Cu[b]	%C[c]	%*trans*[c,d]		TON[e]	TOF (h^{-1})[f]
					F	C		
Cu(I) MOF[g]	1st	24	0.9	20	51	72	23	0.97
	2nd	48		23	55	72	27	0.56
	3th	24		19	62	73	22	0.92
	4th	110		18	54	66	21	0.19
Cu(I) MOF[h]	1st	28	0.9	20	58	73		
	2nd	96		9	46	67		
No catalyst		24		7	57	60		
$CuSO_4$+4,4′-bpy		110	0.9	7	52	66		
CuBox		3	1.0	93	57	71	95	32

[a] Reactions performed at room temperature using 5.00 mmol styrene, 1.80 mmol *n*-undecane (internal standard), 139 mg of MOF and 5.50 mmol of EDA in 10.0 ml of CH_2Cl_2.
[b] Cu molar% relatively to styrene.
[c] Determined by CG-FID.
[d] %*trans* = *trans* × 100/(*trans*+*cis*); *F*=diethyl fumarate, *trans* by-product from the dimerization of EDA (*cis*=diethyl maleate); *C*=cyclopropane.
[e] *TON*=moles of styrene converted/moles of Cu.
[f] *TOF*=*TON*/time of reaction.
[g] Reaction performed without constant stirring.
[h] Reaction performed under constant magnetic stirring at 1000 rpm.

a slightly higher *trans* cyclopropane diastereoselectivity (73%). In the next cycle the reaction slowed down and comparable styrene conversion was achieved only after 110 h with decrease in the *trans* cyclopropane diastereoselectivity (66%).

It is noteworthy that the reaction was also performed under constant stirring conditions with similar catalytic performance as without stirring but in the second cycle the activity was much lower than without stirring, which may be due to the difficult recycling of the crushed MOF crystals.

In the control experiment using comparable amounts of copper(II) sulfate (0.9% mol) and 4,4′-bpy (0.9% mol) as those contained in MOF (1) catalytic reactions styrene conversion after 110 h was similar to the control experiment where no catalyst was used. Hence, the catalytic reactions with (1) were truly heterogeneous and any copper leaching into the solution was not responsible for the observed MOF (1) activity in the cyclopropanation reaction.

It is worth to mention that three copper(I) complexes with 2,2′-bipyridine and styrene were already reported to be homogeneous catalysts in the cyclopropanation of styrene [43]. Cyclopropane diastereoselectivities of 68.2, 69.9 and 82.0, depending on the counterion coordinated and complex structure, can be calculated from the results presented in this paper using a different product analysis methodology. Therefore the present copper(I) MOF is more diastereoselective than most of these reported homogeneous copper(I) complexes.

Clearly, MOF (1) is a heterogeneous catalyst with moderate activity in the cyclopropanation of styrene, high *trans* diastereoselectivity, and it may be recycled and reused at least for three consecutive catalytic cycles with a total turnover number (TON) of 93, similar to the best homogeneous catalyst reported for this reaction (CuBox, Table 4). Although the color of the recycled catalyst is more greenish than the color of the parent material (more yellowish), the PXRD pattern of the former (Fig. 8) shows the presence of (1).

4. Conclusions

This work reports the synthesis, structure and catalytic activity of a new 'hybrid' MOF with mixed organic and inorganic linkers, in the copper-(4,4′-bpy)-sulfate system. With a suitable reductant, L-aspartic acid, we have successfully prepared a Cu(I) supramolecular MOF, $[Cu_2(SO_4)(4,4'\text{-bipy})_2]_4 \cdot 24H_2O$, under mild hydrothermal conditions. The volume (10106.1 $Å^3$) of the unit cell of (1) is relatively considerable, much larger than the volume of a similar structure previously reported [16] (2519.34 $Å^3$) although both materials have the same secondary building unit. The structure of (1) consists of Cu(I) nodes linked by 4,4′-bpy into infinite chains, and sulfate groups connecting two neighboring chains, resulting in a 1-D double chain network. Guest water molecules establish a complicated network of hydrogen bonding interactions with their neighboring oxygen and sulfur atoms, leading to the formation a 3-D supramolecular framework. (1) was tested as a heterogeneous catalyst in the cyclopropanation of styrene showing a high *trans* cyclopropane diastereoselectivity and could be recycled and reused for three consecutive cycles without significant loss of catalytic activity.

Acknowledgments

We acknowledge Fundação para a Ciência e a Tecnologia (FCT) for funding (PTDC/QUI/ 65805/2006, FCOMP-01–0124-FEDER-007424) and Fundo Social Europeu. F.-N. SHI and A.R. Silva acknowledge FCT for Ciência 2007 and 2008 programs, respectively.

Appendix A. Supplementary material

Supplementary material associated with this article can be found in the online version at doi:10.1016/j.jssc.2011.06.023.

References

[1] A.J. Fletcher, K.M Thomas, M.J. Rosseinsky, J. Solid State Chem. 178 (2005) 2491–2510.
[2] D.J. Tranchemontagne, J.L. Mendoza-Cortés, M. O'Keeffe, O.M. Yaghi, Chem. Soc. Rev. 38 (2009) 1257–1283.
[3] O.K Farha, J.T. Hupp, Acc. Chem. Res. 43 (2010) 1166–1175.
[4] J.-P. Zhang, X.-C. Huang, C.-X. Ming, Chem. Soc. Rev. 38 (2009) 2385–2396.
[5] S Natarajan, P. Mahata, Chem. Soc. Rev. 38 (2009) 2304–2318.
[6] H.Y. Yang, L.K. Li, J. Wu, H.W. Hou, B. Xiao, Y.T. Fan, Chem. -Eur. J. 15 (2009) 4049–4056.
[7] J.-R. Li, D.J Timmons, H.-C. Zhou, J. Am. Chem. Soc. 131 (2009) 6368–6369.
[8] Y.-G. Huang, F.-L. Jiang, M.-C. Hong, Coordin. Chem. Rev. 253 (2009) 2814–2834.
[9] X. Gan, W.-F. Fu, Y.-Y. Lin, M. Yuan, C.-M. Che, S.-M. Chi, H.-F. Jie, Li, J.-H. Chen, Y. Chen, Z.-Y. Zhou, Polyhedron 27 (2008) 2202–2208.
[10] A. Almesåker, S.A. Bourne, G. Ramon, J.L. Scott, C.R. Strauss, Cryst. Eng. Commun. 9 (2007) 997–1010.
[11] A.G. Bingham, H. Bögge, A. Müller, E.W. Ainscough, A.M. Brodie, J. Chem. Soc., Dalton Trans. (1987) 493–499.
[12] S.P. Foxon, G.R. Torres, O. Walter, J.Z. Pedersen, H. Toftlund, M. Hüber, K. Falk, W. Haase, J. Cano, F. Lloret, M. Julve, S. Schindler, Eur. J. Inorg.Chem. (2004) 335–343.

[13] W. Zhao, J. Fan, Y. Song, H. Kawaguchi, T. Okamura, W.-Y. Sun, N. Ueyama, Dalton Trans. (2005) 1509–1517.
[14] K. Uemura, A. Maeda, H. Kita, Polyhedron 27 (2008) 2939–2942.
[15] L. Xu, E. Wang, J. Peng, R. Huang, Inorg. Chem. Commun. 6 (2003) 740–743.
[16] N Lah, I. Leban, Inorg. Chem. Commun. 9 (2006) 42–45.
[17] S. Drumel, P. Janvier, M. Bujoli-Doeuff, B. Bujoli, Inorg. Chem. 35 (1996) 5786–5790.
[18] M. Du, Y.-M. Guo, S.-T. Chen, X.-H. Bu, S.R. Batten, J. Ribas, S. Kitagawa, Inorg.Chem. 43 (2004) 1287–1293.
[19] O.A. Bondar, L.V. Lukashuk, A.B. Lysenko, H. Krautscheid, E.B. Rusanov, A.N. Chernega, K.V. Domasevitch, Cryst. Eng. Commun. 10 (2008) 1216–1226.
[20] P. Zhang, Y.-Y. Niu, B.-L. Wu, H.-Y. Zhang, C.-Y. Niu, H.-W. Hou, Inorg. Chim. Acta 361 (2008) 2609–2615.
[21] G. Li, Y. Xing, S. Song, N. Xu, X. Liu, Z. Su, J. Solid State Chem. 181 (2008) 2406–2411.
[22] L.-L. Zheng, J.-D. Leng, S.-L. Zheng, Y.-C. Zhaxi, W.-X. Zhang, M.-L. Tong, Cryst. Eng. Commun. 10 (2008) 1467–1473.
[23] X.-H. Zhou, Y.-H. Peng, X.-D. Du, C.-F. Wang, J.-L. Zuo, X.-Z. You, Cryst. Growth Des. 9 (2009) 1028–1035.
[24] D.A Tocher, M.G.B. Drew, S. Chowdhury, P. Purkayastha, D. Datta, Indian J. Chem. Sect. A 42 (2003) 484–492.
[25] M.J. Ren, J. Zhang, P. Zhao, Z. Zhang, J. Inorg. Organomet. Polym. Mater. 18 (2008) 284–289.
[26] Y.-C. Liu, W.-Y. Yeh, G.-H. Lee, T.-S. Kuo, Inorg. Chim. Acta 362 (2009) 1599–3595.
[27] D. Hagrman, R.P. Hammond, R. Haushalter, J. Zubieta, Chem. Mater. (1998) 2091–2100.
[28] M.-L. Tong, X.-M. Chen, Cryst. Eng. Commun. 2 (2000) 1–5.
[29] B.-Z. Lin, P.-D. Liu, Chin. J. Struct. Chem. 22 (2003) 673–676.
[30] Y. Zhou, J. Yao, W. Liu, K. Yu, Anal. Sci.:X-Ray Struct. Anal. Online 23 (2007) x245–x246.
[31] H. Phetmung, S. Wongsawat, C. Pakawatchai, D.J. Harding, Inorg. Chim. Acta 362 (2009) 2435–2439.
[32] X.-M. Zhang, R.-Q. Fang, H.-S. Wu, S.W. Ng, Acta Cryst. E60 (2004) m990–m992.
[33] D. Farrusseng, S. Aguado, C. Pinel, Angew. Chem. Int. Ed. 48 (2009) 7502–7513.
[34] D.A. Evans, K.A. Woerpel, M.H. Hinman, M.M. Faul, J. Am. Chem. Soc. 113 (1991) 726–728.
[35] G.A. Ardizzoia, S. Brenna, F. Castelli, S. Galli, C. Marelli, A. Maspero, J. Organomet. Chem. 693 (2008) 1870–1876.
[36] J. Vicente, P. González-Herrero, Y. García-Sánchez, P.G. Jones, M. Bardají, Inorg. Chem. 43 (2004) 7516–7531.
[37] APEX2, Data Collection Software Version 2.1-RC13, Bruker AXS, Delft, The Netherlands, 2006.
[38] Cryopad, Remote momitoring and control, Version 1.451, Oxford Cryosystems, Oxford, United Kingdom, 2006.
[39] SAINT^{+}, Data Integration Engine v. 7.23a. Bruker AXS, Madison, Wisconsin, USA, 1997–2005.
[40] G.M. Sheldrick, SADABS v. 2.01, Bruker/Siemens Area Detector Absorption Correction Program, Bruker AXS, Madison, Wisconsin, USA, 1998.
[41] G.M. Sheldrick, SHELXS-97, Program for Crystal Structure Solution, University of Göttingen, 1997.
[42] G.M. Sheldrick, SHELXL-97, Program for Crystal Structure Refinement, University of Göttingen, 1997.
[43] C. Ricardo, T. Pintauer, J. Organomet. Chem. 692 (2007) 5165–5172.